Hydrogen bond, electron donor-acceptor dimer, and residence dynamics in supercritical CO_2-ethanol mixtures and the effect of hydrogen bonding on single reorientational and translational dynamics: A molecular dynamics simulation study

Ioannis Skarmoutsos,[1,a)] Elvira Guardia,[2,b)] and Jannis Samios[3,c)]
[1]*Department of Chemistry, Imperial College London, London SW7 2AZ, United Kingdom*
[2]*Departament de Física i Enginyeria Nuclear, Universitat Politècnica de Catalunya, B4-B5 Campus Nord UPC, Barcelona, Catalonia 08034, Spain*
[3]*Department of Chemistry, Laboratory of Physical Chemistry, University of Athens, Panepistimiopolis, Athens 157-71, Greece*

(Received 29 March 2010; accepted 19 May 2010; published online 7 July 2010)

The hydrogen bonding and dynamics in a supercritical mixture of carbon dioxide with ethanol as a cosolvent ($X_{ethanol} \sim 0.1$) were investigated using molecular dynamics simulation techniques. The results obtained reveal that the hydrogen bonds formed between ethanol molecules are significantly more in comparison with those between ethanol-CO_2 molecules and also exhibit much larger lifetimes. Furthermore, the residence dynamics in the solvation shells of ethanol and CO_2 have been calculated, revealing much larger residence times for ethanol molecules in the ethanol solvation shell. These results support strongly the ethanol aggregation effects and the slow local environment reorganization inside the ethanol solvation shell, reported in a previous publication of the authors [Skarmoutsos *et al.*, J. Chem. Phys. **126**, 224503 (2007)]. The formation of electron donor-acceptor dimers between the ethanol and CO_2 molecules has been also investigated and the calculated lifetimes of these complexes have been found to be similar to those corresponding to ethanol-CO_2 hydrogen bonds, exhibiting a slightly higher intermittent lifetime. However, the average number of these dimers is larger than the number of ethanol-CO_2 hydrogen bonds in the system. Finally, the effect of the hydrogen bonds formed between the individual ethanol molecules on their reorientational and translational dynamics has been carefully explored showing that the characteristic hydrogen bonding microstructure obtained exhibits sufficiently strong influence upon the behavior of them. © *2010 American Institute of Physics*. [doi:10.1063/1.3449142]

I. INTRODUCTION

It is well known for the past years that some limitations in the use of the green nontoxic solvent supercritical (sc) CO_2 in order to dissolve polar organic solutes and dyes have been significantly reduced by the addition of polar cosolvents in sc CO_2.[1–8] Furthermore, by selecting the proper polar cosolvent the selective dissolution of several molecular species could be appropriately tuned, thus making these binary solvents widely used in extraction and separation techniques,[9,10] as well as suitable media for specific chemical reactions under sc conditions.[11–13] The most common cosolvents used for these purposes are the lower alcohols (methanol, ethanol, 2-propanol, etc.) and they have been widely employed in a wide range of important applications in material science.[14–17] Therefore, the investigation of the structural and dynamic properties of these mixed solvents becomes necessary in order to reveal important information about their characteristic behavior.

Although a small number of experimental and theoretical studies devoted to the properties of sc CO_2-methanol mixed solvents (with $X_{methanol} \sim 0.01-0.11$) have been reported up to now,[18–29] studies on the properties of scCO_2-ethanol (EtOH) systems are quite rare and most of them correspond mainly to dilute mixtures.[24,30–37] In a quite recent study, two of the authors presented a molecular dynamics (MD) simulation study on the local intermolecular structure and related dynamics for the sc CO_2–EtOH binary mixture at a mole fraction $X_{ethanol} \sim 0.1$.[36] The results obtained in that study have revealed a nonideal mixing behavior of the mixture and the existence of a somewhat restricted aggregation between the ethanol molecules. This effect has been also observed in the case of sc CO_2–MeOH mixture and reported by us in the framework of a recent MD study of the system.[18]Furthermore, the local environment redistribution dynamics revealed that the time dependent redistribution of the first solvation shell of ethanol is much slower in comparison with the first shell of CO_2 and this observation has been interpreted in terms of the existence of weaker interactions between the CO_2–CO_2 and EtOH–CO_2 molecules in comparison with the EtOH–EtOH ones, which could be a result of stronger hydrogen bonding (HB) interactions. Moreover, another recent Monte Carlo simulation study[37] has revealed that the EtOH–EtOH HB network is the most im-

[a)]Electronic mail: i.skarmoutsos@imperial.ac.uk.
[b)]Electronic mail: elvira.guardia@upc.edu.
[c)]Electronic mail: isamios@chem.uoa.gr.

portant in these mixtures, having as a result the appearance of aggregates between the EtOH molecules in the fluid.

However, the investigation of the dynamics of these hydrogen bonds has not been presented in any study so far. Therefore, in the present treatment we decide to investigate in details the dynamics of the hydrogen bonds formed between the EtOH molecules and to compare them with the EtOH–CO_2 HB dynamics in order to seek for any possible interrelations of these dynamics with the local environment reorganization. Moreover, taking into account that in many cases the dynamics of local solvation and aggregation effects in molecular fluids have been also interpreted in terms of the residence dynamics, we decided to investigate also these dynamics for the first solvation shell of EtOH and CO_2 molecules. The investigation of possible resemblances and differences between all these relaxation processes could provide important information concerning several factors affecting local aggregation dynamics in molecular fluids.

At this point we have to mention that previously reported experimental and theoretical studies have revealed that the addition of alcohols, which act as Lewis bases, in CO_2 (which exhibits an acid behavior through the carbon atom) leads to the observation of a Lewis acid-base-type interaction and to the formation of an electron donor-acceptor (EDA) dimer.[30,35,37,38] In a previous Monte Carlo simulation study Xu *et al.*[37] proposed a geometric criterion and performed a static analysis of EDA dimers in EtOH–CO_2 mixtures. According to the results obtained in that study, the EDA EtOH–CO_2 dimer is more stable than the hydrogen bonded one. This observation was based on the calculated relative energies of the EDA and HB dimers. However, a more detailed analysis of the stability of the EDA and HB dimers could be achieved only by investigating the dynamics of these interactions. For this reason, we decided to calculate the HB and EDA dimer dynamics and the corresponding lifetimes in order to extract more information about the stability of these complexes.

Finally, one of the aims in the present study is to explore systematically also the effect of the HB state of the individual ethanol molecules on their single dynamic properties. More specifically, in the present treatment we have focused on the effect of the presence of hydrogen bonds on the reorientational and translational dynamics of the EtOH molecules and how the strength of these HB interactions might affect these molecular motions in the fluid.

This paper is organized as follows. The computational details of the performed simulations are presented in Sec. II. The results obtained and the following discussion upon them are presented in Sec. III. Finally, Sec. IV contains the general conclusions and remarks drawn from the present study.

II. COMPUTATIONAL DETAILS

In the present treatment we performed a MD simulation of a mixture consisted of 48 ethanol and 452 CO_2 molecules in the central simulation box, employing also periodic boundary conditions. The simulation was performed at constant temperature and volume, corresponding to an experimentally reported sc thermodynamic state point ($T=348$ K, $\rho=0.611$ g/cm^3).[31] According to previous experimental studies the critical temperature of the mixture at this particular composition has estimated to be about 326 K,[31,36] therefore the investigated fluid mixture is at sc conditions. The intermolecular interactions are represented as pairwise additive with site-site Lennard-Jones (LJ) and Coulombic interactions. In the case of different interaction sites, the Lorentz–Berthelot combining rules were used. The minimum image convention was also employed for the calculation of the intermolecular forces. The EPM2 force field[39] was used to describe the site-site interactions of CO_2 and the flexible Optimized Potentials for Liquid Simulations-United Atom (OPLS-UA) (Ref. 40) was employed for EtOH. In the flexible OPLS-UA potential, the intramolecular torsion around the central C_2–O bond has been expressed by using the following dihedral angle potential:

$$U(\varphi) = U_0 + \tfrac{1}{2}U_1(1+\cos\varphi) + \tfrac{1}{2}U_2(1-\cos 2\varphi) + \tfrac{1}{2}U_3(1+\cos 3\varphi). \quad (1)$$

These force fields have been used successfully in several simulations of both pure EtOH and CO_2 at liquid and sc conditions[41–48] as well as in sc methanol-CO_2 mixtures[18] and other binary sc mixtures.[49]

The system was simulated for 300 ps in order to achieve equilibration and the properties of interest were calculated by analyzing the trajectories of a subsequent 400 ps simulation after the equilibration period. A leapfrog-type Verlet algorithm was used for the integration of the equations of motion using a time step of 1 fs. The temperature of the system was constrained using the Berendsen thermostat[50] with a temperature relaxation of 0.5 fs. The intramolecular geometry of the molecules was constrained during the simulations by using the shake algorithm.[51] In each simulation, a cutoff radius of 1.2 nm was used to all LJ interactions and long-range corrections have been also taken into account. Moreover, the Ewald summation technique, with the use of the more exact approximation Newton–Gregory forward difference interpolation scheme, was applied to account for the long-range electrostatic interactions.[52]

III. RESULTS AND DISCUSSION

A. HB and EDA dimer statics and dynamics

In a previous study reported by the authors,[36] the calculated O–H, O–O, and H–H EtOH–EtOH site-site radial distribution function had revealed the possible existence of hydrogen bonds between the ethanol molecules. Moreover, the calculation of the local mole fractions around ethanol had revealed a significant composition enhancement of ethanol around a central ethanol molecule, thus signifying the existence of ethanol aggregates in the mixture. The calculated EtOH–CO_2 radial distribution functions had supported previously mentioned experimental and *ab initio* findings indicating a weak complex structure between EtOH and CO_2. It is interesting to note that the intermolecular distance O(EtOH)$\cdots$C(CO_2) for this weak complex calculated in our previous study[36] has been found to be in very good agree-

TABLE I. Average number of formed hydrogen bonds per ethanol molecule and fraction of ethanol molecules forming 0,1,2,3 hydrogen bonds of each type.

Type of H bond	$100f_0$ (%)	$100f_1$ (%)	$100f_2$ (%)	$100f_3$ (%)	$\langle n_{HB} \rangle$
EtOH–EtOH	44.72	32.48	22.20	0.60	0.79
EtOH–CO_2	86.93	13.05	1.73	0.02	0.13

ment with the results of previously reported *ab initio* studies.[30,38]

Taking into account all the above mentioned arguments, we decided to perform a more detailed analysis of hydrogen bonds and EDA dimers in the system, including not only a static but also a dynamic description of these structures. To do so, we have performed a HB analysis based on previously widely used simple geometric criteria. According to the criterion used in our study, a hydrogen bond between two EtOH molecules exists if the intermolecular distances are $R_{O\cdots O} \leq 3.5$ Å, $R_{H\cdots O} \leq 2.6$ Å and the donor-acceptor angle $\phi \equiv H\text{–}O\cdots O \leq 30°$ ($\cdots$ denotes an intermolecular vector, whereas – denotes an intramolecular one). This criterion has been successfully used in previous studies of alcohols[41,43–45] and CO_2-alcohol mixtures.[18,37,53] In order to investigate the existence of hydrogen bonds between EtOH and CO_2 we also employed a geometric criterion, according to which a hydrogen bond between an EtOH and CO_2 molecule exists if the intermolecular distances are $R_{O\cdots O} \leq 3.5$ Å, $R_{H\cdots O} \leq 2.6$ Å and the donor-acceptor EtOH–CO_2 angle $\phi \equiv H\text{–}O\cdots O(CO_2) \leq 30°$. The calculated average number of each type of hydrogen bond per ethanol molecule as well as the fractions of ethanol molecules having 0, 1, 2, and 3 hydrogen bonds of each type are presented in Table I. From these results we may see that the number of hydrogen bonds between EtOH molecules is significantly larger than that one corresponding to EtOH–CO_2 hydrogen bonds. Similar findings have been observed in the case of methanol-CO_2 mixtures, as well as in the Monte Carlo investigation of Xu *et al.*[37] mentioned in Sec. I. In order to obtain also a picture of the geometrical characteristics of the hydrogen bonds formed among the ethanol molecules, as well as those formed between EtOH and CO_2 ones, we have calculated the hydrogen bond length $R_{H\cdots O}$ and bond angle ϕ distributions between these pairs of molecules. The selected angles ϕ are the angles used in the HB criteria. In the framework of the present study we calculated the distribution of angles ϕ_{ij} for pairs of molecules having only $R_{O\cdots O} \leq 3.5$ Å and $R_{H\cdots O} \leq 2.6$ Å. The results obtained are presented in Fig. 1(a), revealing that in the case of EtOH–EtOH the donor-acceptor angle ϕ is in general smaller, supporting further the fact that EtOH–EtOH hydrogen bonds are stronger than EtOH–CO_2 ones.

In the case of the EDA dimers, we performed an analysis using the geometric criterion of Xu *et al.*,[37] according to which an EDA dimer between an EtOH and CO_2 molecule exists if the intermolecular distances are 2.6 Å $\leq r_{C(CO_2)\cdots O} \leq 4.3$ Å, and the EtOH–CO_2 donor-acceptor angles are $85° \leq \theta_1 \leq 130°$ and $90° \leq \theta_2 \leq 140°$, where $\theta_1 \equiv H\text{–}O\cdots C(CO_2)$ and $\theta_2 \equiv C_2\text{–}O\cdots C(CO_2)$ (C_2 corresponds to the CH_2-unified site of OPLS-UA ethanol). In order to investigate the effect of the geometric criteria on the calculation we also employed the geometric criterion suggested in a Car–Parinello study[35] on the solvation of an EtOH molecule in sc CO_2. According to this criterion[35] an EDA dimer between an EtOH and CO_2 molecule exists if the intermolecular distances are $r_{C(CO_2)\cdots O} \leq 4.3$ Å and $90° \leq \theta_1, \theta_2 \leq 130°$. The results obtained by our analysis using both criteria are presented in Table II. From these results we may say that the second criterion predicts a slightly smaller number of EDA dimers per ethanol molecule. This may be easily explained by presenting the distribution of angles θ_1, θ_2 for EtOH–CO_2 pairs having 2.6 Å $\leq r_{C(CO_2)\cdots O} \leq 4.3$ Å in Fig. 1(b), where we may see that a larger percentage of EtOH–CO_2 pairs are in the range of angles defined by the first criterion. In comparison with the EtOH–CO_2 hydrogen

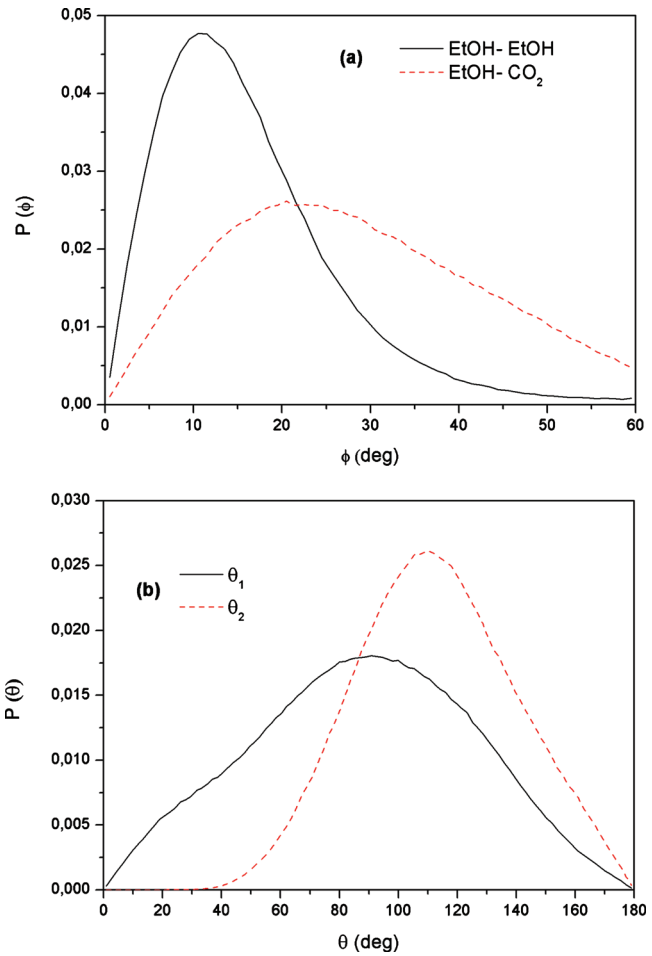

FIG. 1. (a) Distribution of angles ϕ_{ij} for pairs of molecules having only $R_{O\cdots O} \leq 3.5$ Å and $R_{H\cdots O} \leq 2.6$ Å. (b) Distribution of angles θ_1, θ_2 for EtOH–CO_2 pairs having 2.6 Å $\leq r_{C(CO_2)\cdots O} \leq 4.3$ Å.

TABLE II. Average number of formed EDA dimers per ethanol molecule and fraction of ethanol molecules forming 0,1,2,3 EDA dimers using two different geometric definitions.

EDA dimer	$100f_0$ (%)	$100f_1$ (%)	$100f_2$ (%)	$100f_3$ (%)	$\langle n_{EDA} \rangle$
Criterion 1	62.97	32.24	4.70	0.09	0.42
Criterion 2	71.63	25.75	2.59	0.03	0.31

bonds, we may see that in both cases the number of EDA dimer is higher than the number of EtOH–CO_2 HB pairs. This fact signifies that the EDA interactions between EtOH and CO_2 molecules in the mixture are possibly more important than the HB ones. This finding comes in agreement with previous experimental spectroscopic studies as well as the *ab initio*[30,38] and Monte Carlo[37] studies. In general we have observed that $\langle n_{HB} \rangle_{EtOH-EtOH} > \langle n_{EDA} \rangle_{EtOH-CO_2} > \langle n_{HB} \rangle_{EtOH-CO_2}$, which could be used in order to classify the importance of several types of interactions in the mixture. However, a more detailed analysis of the stability interactions can be provided only by analyzing the dynamics of these interacting pairs in the mixture. Therefore, in the present study we decided to calculate the dynamics of the EtOH–EtOH and EtOH–CO_2 hydrogen bonds as well as the dynamics of the EtOH–CO_2 EDA complexes in order to reveal more information regarding the nature of these different types of interactions.

The dynamics of hydrogen bonds in the mixture have been studied by calculating the well-known HB time correlation function (tcf) for the pairs i,j of hydrogen bonded molecules defined as

$$C_{HB}(t) = \frac{\langle h_{ij}(0) \cdot h_{ij}(t) \rangle_{t^*}}{\langle h_{ij}(0)^2 \rangle}. \quad (2)$$

The corresponding HB lifetime is defined as

$$\tau_{HB} = \int_0^\infty C_{HB}(t) \cdot dt. \quad (3)$$

The variable h_{ij} has been defined in the following way:

$$h_{ij}(t) = 1,$$

if molecule j is hydrogen bonded with molecule i at times 0 and t and the bond has not been broken in the meantime for a period longer than t^*,

$$h_{ij}(t) = 0, \text{ otherwise}. \quad (4)$$

Of course, according to this definition, the calculation of $C_{HB}(t)$ depends upon the selection of the parameter t^*. The two limiting cases arising from this definition are the following.

(a) If $t^*=0$, which represents the so-called continuous definition. In this case the calculated tcf is the continuous one $C_{HB}{}^C(t)$ and the corresponding lifetime is the continuous lifetime $\tau_{HB}{}^C$.

(b) If $t^*=\infty$, which represents the so-called intermittent definition. In this case the calculated tcf is the intermittent one $C_{HB}{}^I(t)$ and the corresponding lifetime is the intermittent lifetime (or HB relaxation time) $\tau_{HB}{}^I$.

We have to mention that these two definitions describe very different aspects of HB dynamics and have been extensively discussed in previous publications. In the framework of the present study we calculated the continuous and intermittent HB lifetimes for the EtOH–EtOH and EtOH–CO_2 hydrogen bonds and these function are depicted in Figs. 2 and 3. The calculated continuous and intermittent HB lifetimes are also presented in Table III. From the results obtained we may clearly see that the HB lifetimes are significantly larger in the case of EtOH–EtOH hydrogen bonds in comparison with the lifetimes of the EtOH–CO_2 ones, especially in the case of intermittent dynamics. This is clear evidence that there is a much stronger correlation between the hydrogen bonded EtOH molecules than between the hydrogen bonded EtOH and CO_2 ones. Therefore, we then focused

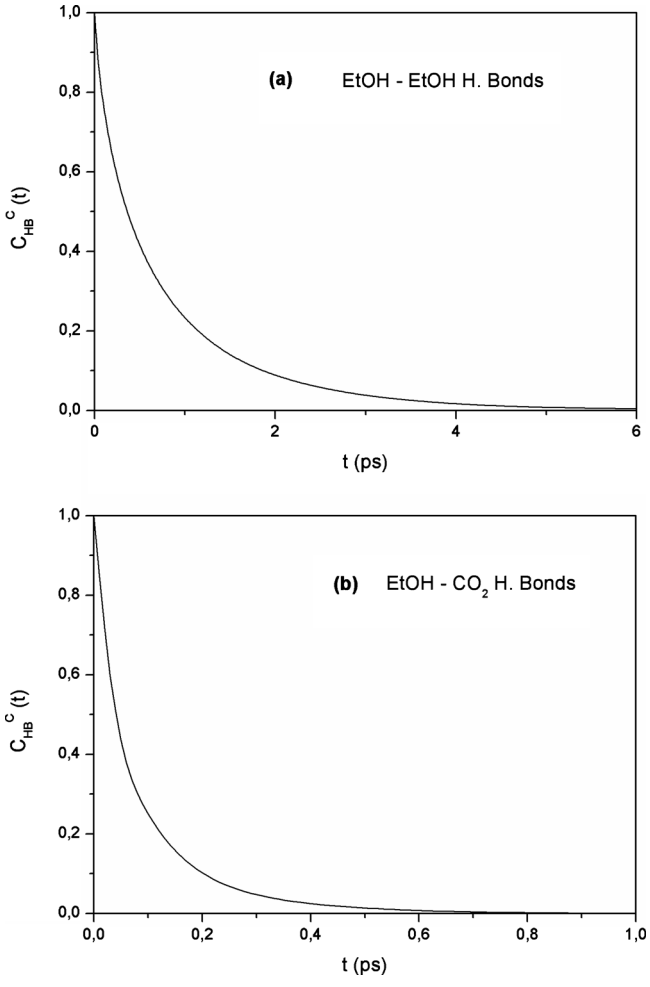

FIG. 2. Continuous HB correlation functions for EtOH–EtOH and EtOH–CO_2 H bonds.

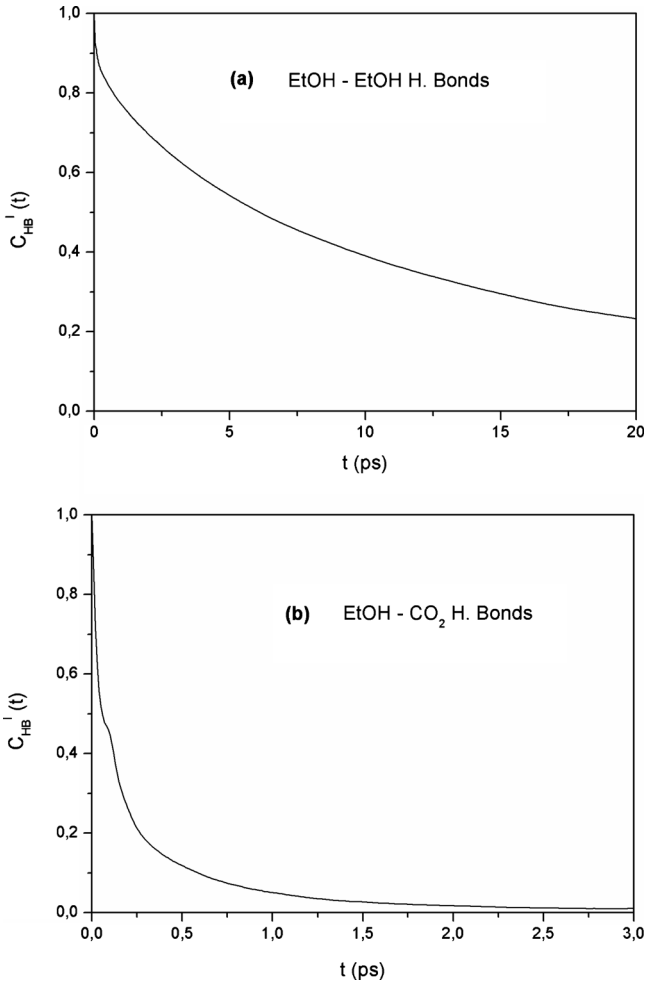

FIG. 3. Intermittent HB correlation functions for EtOH–EtOH and EtOH–CO_2 H bonds.

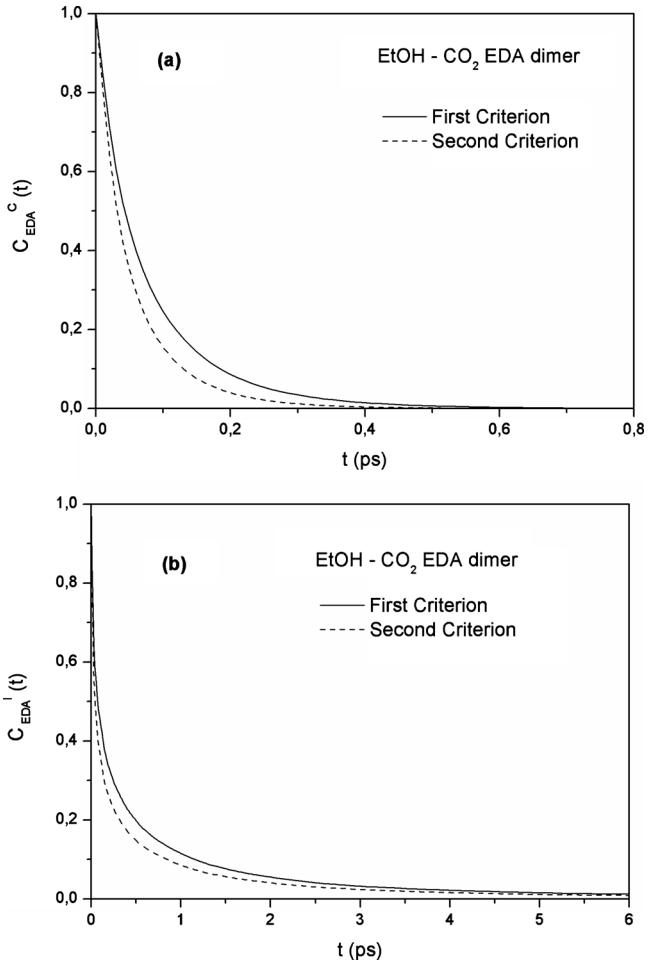

FIG. 4. Continuous and intermittent EDA correlation functions for EtOH–CO_2 dimers using two different geometric criteria.

our attention on the investigation of the relative stabilities between the hydrogen bonded and EDA EtOH–CO_2 dimers.

In this particular case, the dynamics of EDA dimers have been studied using the same formalism as in the case of HB dynamics. Therefore, the EDA tcf has been defined as

$$C_{\mathrm{EDA}}(t) = \frac{\langle k_{ij}(0) \cdot k_{ij}(t) \rangle_{t^*}}{\langle k_{ij}(0)^2 \rangle}. \tag{5}$$

The variable k_{ij} has been defined in the following way:

TABLE III. Continuous and intermittent HB lifetimes for EtOH–EtOH and EtOH–CO_2 H bonds.

Type of H bond	τ_{HB}^{C} (ps)	τ_{HB}^{I} (ps)
EtOH–EtOH	0.73	13.20
EtOH–CO_2	0.08	0.26
EDA dimer	τ_{EDA}^{C} (ps)	τ_{EDA}^{I} (ps)
Criterion 1	0.08	0.51
Criterion 2	0.05	0.39

$$k_{ij}(t) = 1,$$

if a CO_2 molecule j forms an EDA dimer with an EtOH molecule i at times 0 and t and the dimer structure has not been broken in the meantime for a period longer than t^*,

$$k_{ij}(t) = 0, \quad \text{otherwise}. \tag{6}$$

In an analogous way with HB dynamics, we have calculated the continuous ($t^*=0$) and intermittent ($t^*=\infty$) tcf's. Note that we have calculated these functions using both the aforementioned geometric criteria for the estimation of EDA and the results are depicted in Fig. 4. Furthermore, we have calculated the corresponding lifetimes (presented in Table III) of the EDA dimers using the relation

$$\tau_{\mathrm{EDA}} = \int_0^{\infty} C_{\mathrm{EDA}}(t) \cdot dt. \tag{7}$$

From the results obtained we may see that the criteria do not affect significantly the dynamics of the EDA dimers. In comparison with the dynamics of the EtOH–CO_2 hydrogen bonded dimers we may conclude that in the case of continuous dynamics the calculated lifetimes are quite similar, but in the case of intermittent dynamics the lifetimes of the EDA dimers are larger than those of the hydrogen bonded ones. This finding indicates that the correlation between EDA

dimers is stronger than in the case of the hydrogen bonded ones. In general the tendency concerning the lifetimes of all interacting dimers is $\langle \tau_{HB}{}^{C} \rangle_{EtOH-EtOH} > \langle \tau_{EDA}{}^{C} \rangle_{EtOH-CO_2} \cong \langle \tau_{HB}{}^{C} \rangle_{EtOH-CO_2}$ and $\langle \tau_{HB}{}^{I} \rangle_{EtOH-EtOH} \gg \langle \tau_{EDA}{}^{I} \rangle_{EtOH-CO_2} > \langle \tau_{HB}{}^{I} \rangle_{EtOH-CO_2}$. This outcome, together with the finding concerning the average number of the different types of interacting dimers in the system, clearly indicates that the EtOH–EtOH HB dimers are the most stable in the system and the EDA EtOH–CO_2 dimers are more stable than the EtOH–CO_2 HB ones.

Since the dynamics of EtOH–EtOH hydrogen bonds are significantly slower in comparison with those of EtOH–CO_2 bonds (hydrogen bonds or EDA dimers), we decided to investigate further the dynamics of EtOH molecules at different HB states. The continuous HB state dynamics can be investigated by calculating the function

$$C_{HB}{}^{n,C}(t) = \frac{\langle h_n^C(0) \cdot h_n^C(t) \rangle}{\langle h_n^C(0)^2 \rangle}. \quad (8)$$

The variable $h_n^C(t)$ has been defined as follows:

$$h_n^C(t) = 1,$$

if an ethanol molecule forms continuously in the time period $\Delta t = 0 \rightarrow t$ n hydrogen bonds (is in the n HB state) with other ethanol molecules,

$$h_n^C(t) = 0, \text{ otherwise}. \quad (9)$$

The intermittent HB state dynamics have been investigated by calculating the function

$$C_{HB}{}^{n,I}(t) = \frac{\langle \delta h_n^I(0) \cdot \delta h_n^I(t) \rangle}{\langle \delta h_n^I(0)^2 \rangle}, \quad \delta h_n^I(t) = h_n^I(t) - \langle h_n^I \rangle. \quad (10)$$

The variable $h_n^I(t)$ has been defined in the following way:

$$h_n^I(t) = 1,$$

if an ethanol molecule that was in the HB state n at time $t=0$ is in the same HB state at time t, independent of whether or not its HB state has changed in the meantime,

$$h_n^I(t) = 0, \text{ otherwise}. \quad (11)$$

The corresponding lifetimes have been defined as

$$\tau_{HB}{}^{n,C} = \int_0^\infty C_{HB}{}^{n,C}(t) \cdot dt$$

and

$$\tau_{HB}{}^{n,I} = \int_0^\infty C_{HB}{}^{n,I}(t) \cdot dt. \quad (12)$$

The calculated functions defined in Eqs. (7) and (9) for the HB states $n=0,1,2$ are presented in Fig. 5 and the corresponding lifetimes in Table IV. We have to note that in order to calculate the HB state lifetimes we fitted a sum of three exponential decay functions to the calculated tcf's. Therefore, in order to estimate the lifetimes, we calculated the numerical integrals up to 30 ps and the rest was calculated by obtaining analytically the integrals for the tails corresponding to time scales larger than 30 ps using the fitting functions. By inspecting carefully these results we may see that the continuous lifetime for a HB free EtOH molecule ($n=0$ HB state) is much larger in comparison with the continuous lifetimes of EtOH molecules in the $n=1$ and $n=2$ HB states (8.95, 0.52, and 0.35 ps, respectively). However, it is very interesting that this behavior changes in the case of intermittent dynamics and the intermittent lifetimes of HB free EtOH molecules and those in the $n=2$ HB state are quite similar ($\tau_{HB}{}^{0,I}=12.3$ ps and $\tau_{HB}{}^{2-I}=9.4$ ps) and much larger than the intermittent lifetime of molecules in the $n=1$ HB state ($\tau_{HB}{}^{1-I}=3.1$ ps). By inspecting the correlation functions in Fig. 5(b), we may see that the decay of $C_{HB}{}^{2,I}(t)$ starts to become slower than that of $C_{HB}{}^{0,I}(t)$ at larger time scales. This result indicates that the formation of larger HB complexes between EtOH molecules leads to a stronger correlation between them and therefore to higher intermittent lifetimes. Therefore, it is very likely that the

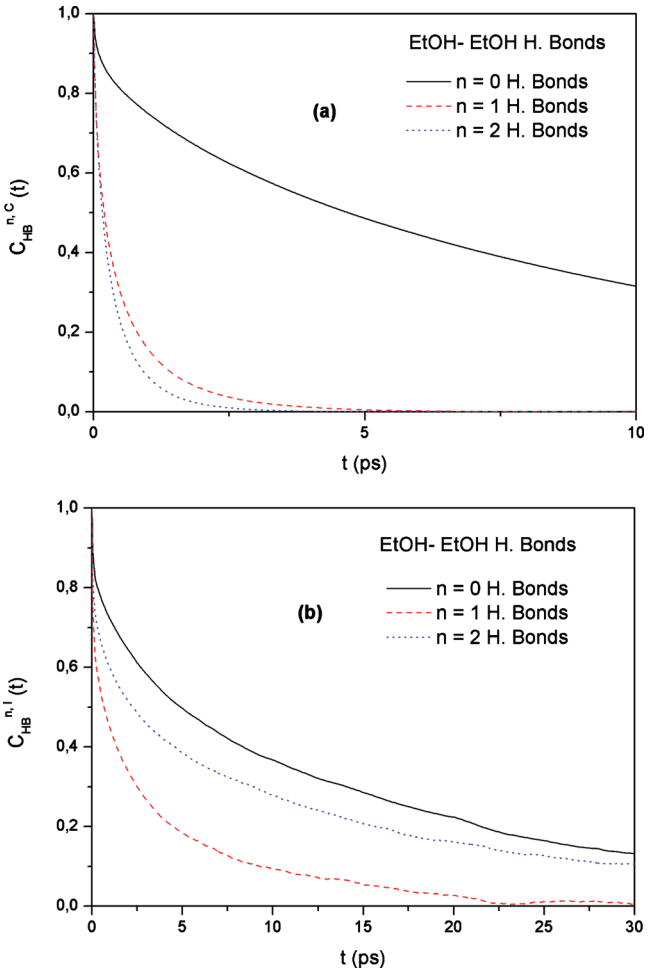

FIG. 5. Continuous and intermittent HB state correlation functions for EtOH–EtOH H bonds and for the HB states $n=0,1,2$.

TABLE IV. Continuous and intermittent lifetimes for EtOH molecules in the HB states $n=0,1,2$ (only for EtOH–EtOH H bonds).

	$n=0$	$n=1$	$n=2$
$\tau_{HB}{}^{n,C}$ (ps)	8.95	0.52	0.35
$\tau_{HB}{}^{n,I}$ (ps)	12.30	3.10	9.40

higher lifetimes for strongly H-bonded EtOH complexes retard the reorganization of the local environment around the EtOH molecules. This result supports further our previous observations[36] regarding the slow reorganization of the local environment around the EtOH molecules in comparison to the much faster reorganization of the local environment around CO_2.

B. Residence dynamics

Besides the HB and EDA dimer dynamics, in the present treatment we have also investigated the residence dynamics of the molecules in the first solvation shells of EtOH and CO_2, since residence dynamics provides an alternative way to investigate dynamic local aggregation effects in molecular fluids. The residence tcf inside a solvation shell around a central particle i could be defined as follows:

$$C_{\mathrm{res}}(t) = \frac{\langle n_{ij}(0) \cdot n_{ij}(t) \rangle_{t^*}}{\langle n_{ij}(0)^2 \rangle}. \tag{13}$$

The corresponding residence time is defined according to the following relation:

$$\tau_{\mathrm{res}} = \int_0^\infty C_{\mathrm{res}}(t) \cdot dt. \tag{14}$$

The variable n_{ij} has been defined in the following way:

$$n_{ij}(t) = 1,$$

if molecule j is inside the solvation shell of molecule i at times 0 and t and the molecule j has not left in the meantime the shell for a period longer than t^*,

$$n_{ij}(t) = 0, \text{ otherwise}. \tag{15}$$

In the present treatment, we have calculated the continuous residence tcf ($t^*=0$) as well as a tcf obtained by using a $t^*=2$ ps value. The tcf's were calculated for the EtOH and CO_2 molecules inside the solvation shells of EtOH and CO_2, respectively. The positions of the solvation shells corresponding to the center of mass EtOH–EtOH, EtOH–CO_2, and CO_2–CO_2 radial distribution functions were calculated in our previous study[36] and were used in this study to define the cutoff distances of the shells. The calculated residence tcf's are depicted in Figs. 6 and 7 and the calculated residence times are summarized in Table V. From the results obtained we may see that the residence times of EtOH molecules inside an EtOH solvation shell are much larger in comparison to all the other calculated lifetimes, whereas the lifetimes of CO_2 inside a CO_2 solvation shell are the smallest ones. This result seems to be reasonable taking into account all our above mentioned findings concerning HB dynamics.

Moreover, in a previous treatment[36] we had calculated the local environment reorganization tcf's of the instantaneous local coordination number deviation relative to the mean local one ($\delta N_{ij}(t) = N_{ij}(t) - \langle N_{ij} \rangle$) for a fixed cutoff distance that specified the volume of the first solvation shell around an EtOH or CO_2 molecule. By performing this analysis we had found that the time required for the redistribution of the local environment around the EtOH molecules is quite larger in comparison to the one corresponding to the redistribution of the local environment around CO_2. Furthermore, by analyzing in details the local environment reorganization tcf for the solvation shell of EtOH we pointed out that the reorganization of this shell is mainly determined by the redistribution of the CO_2 molecules. Our findings in the present study can easily explain this observation. Due to the stronger EtOH–EtOH interactions the EtOH molecules inside a solvation shell stay bound together for a significant time scale, whereas the weaker EtOH–CO_2 dimers break more rapidly and therefore the CO_2 molecules are more free to exit and reenter the solvation shell of ethanol. This is very clearly reflected on the calculated residence times supporting all these assumptions. Therefore, for the present study it becomes very clear that the strong EtOH–EtOH interactions affect a wide range of the properties of the mixture.

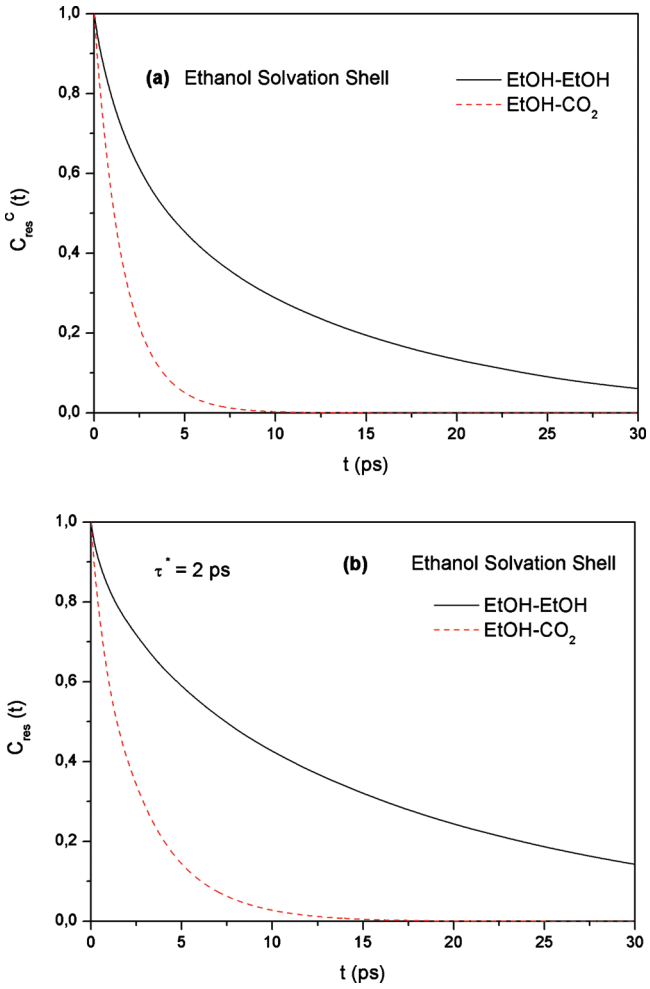

FIG. 6. Residence correlation functions for the molecules in the first solvation shell of EtOH.

C. Reorientational dynamics

Since all our aforementioned results have signified a strong EtOH–EtOH interaction in the mixture we decided to extend our investigations in order to study the effect of these EtOH–EtOH hydrogen bonds on the single dynamic properties of the EtOH molecules. More specifically, we focused on the effect of the EtOH–EtOH hydrogen bonds on the reori-

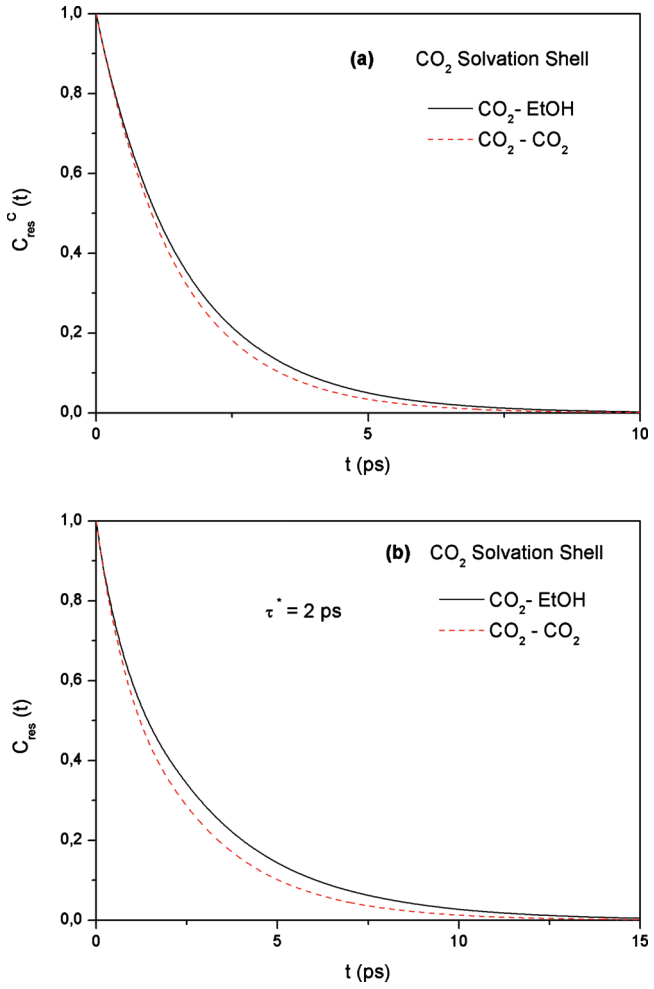

FIG. 7. Residence correlation functions for the molecules in the first solvation shell of CO_2.

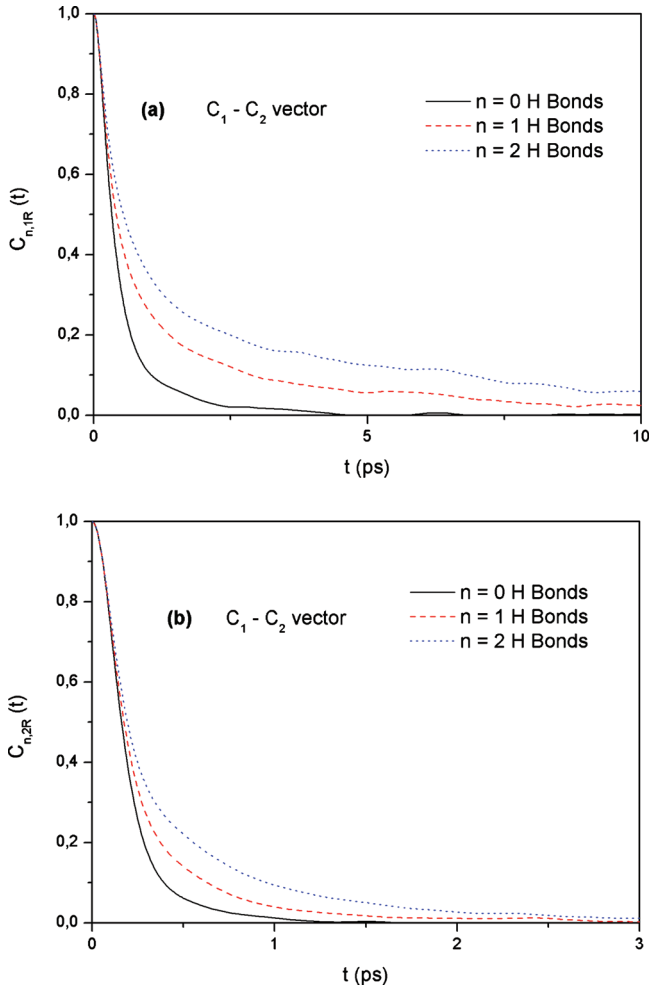

FIG. 8. First and second order Legendre reorientational correlation functions for the C_1-C_2 vector of EtOH molecules corresponding to the initial HB states $n=0,1,2$ (for EtOH–EtOH H bonds).

entational dynamics of several specific intramolecular vectors of EtOH molecules by calculating the appropriate tcf's,[43,54]

$$C_{n,\ell R}(t) = \frac{\langle P_\ell(\vec{u}(0)\cdot\vec{u}(t))\cdot\Theta_n(0)\rangle}{\langle\Theta_n(0)\rangle} \quad n=0,1,2$$

and

$$\ell = 1,2. \tag{16}$$

As previously, the index ℓ defines the order of the Legendre polynomial, whereas the index n defines the instantaneous number of hydrogen bonds which form a molecule at each time t.

The function $\Theta_n(t)$ is defined as follows:

TABLE V. Residence times (continuous and for $t^*=2$ ps) for molecules in the solvation shell of EtOH and CO_2.

i-j pair	τ_{res}^C (ps)	τ_{res} (ps) ($t^*=2$ ps)
EtOH–EtOH	8.74	13.77
EtOH–CO_2	1.63	2.45
CO_2–CO_2	1.47	2.04
CO_2–EtOH	1.63	2.45

$$\Theta_n(t) = 1,$$

if an EtOH molecule forms n EtOH–EtOH hydrogen bonds at time t,

$$\Theta_n(t) = 0, \text{ otherwise.} \tag{17}$$

The corresponding reorientational times are defined as

$$\tau_{n,\ell R} = \int_0^\infty C_{n,\ell R}(t)\cdot dt, \quad n=0,1,2$$

and

$$\ell = 1,2. \tag{18}$$

Therefore, we investigated the reorientational dynamics of molecules forming $n=0$ (free molecules), $n=1$, and $n=2$ hydrogen bonds in order to see the effect of the local HB network on these properties. This analysis was performed for three representative vectors of each of the aforementioned vector groups, namely, the three intramolecular bond vectors C_1-C_2, C_2-O, and O–H. The calculated reorientational tcf's for all the aforementioned vectors and initial HB states are presented in Figs. 8–10 and the corresponding reorientational times are presented in Table VI. From the results obtained we may clearly see that the initial HB state of the EtOH mol-

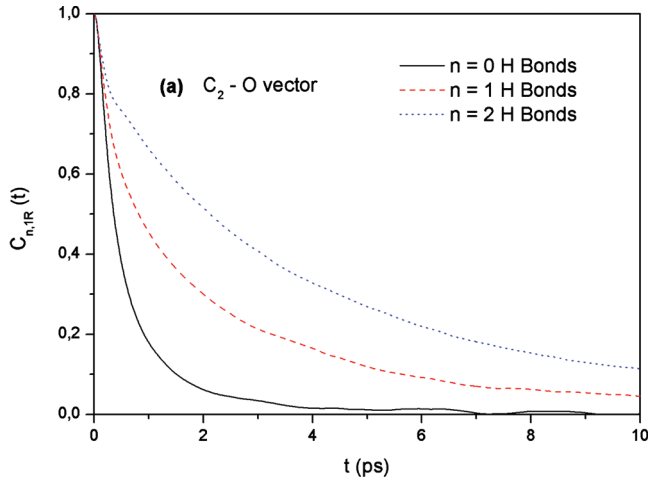

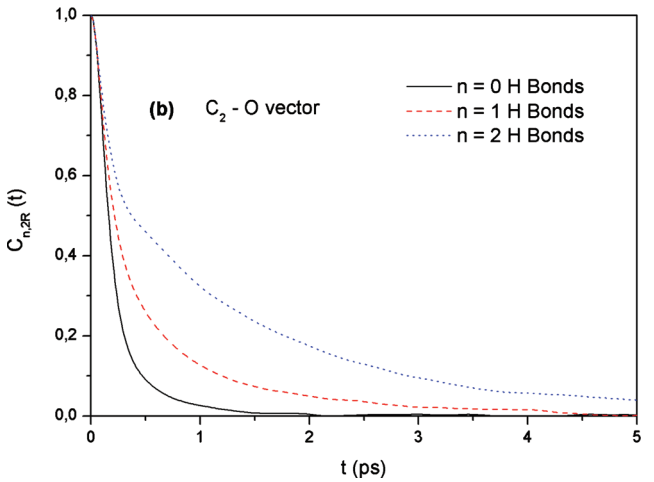

FIG. 9. First and second order Legendre reorientational correlation functions for the C_2-O vector of EtOH molecules corresponding to the initial HB states $n=0,1,2$ (for EtOH–EtOH H bonds).

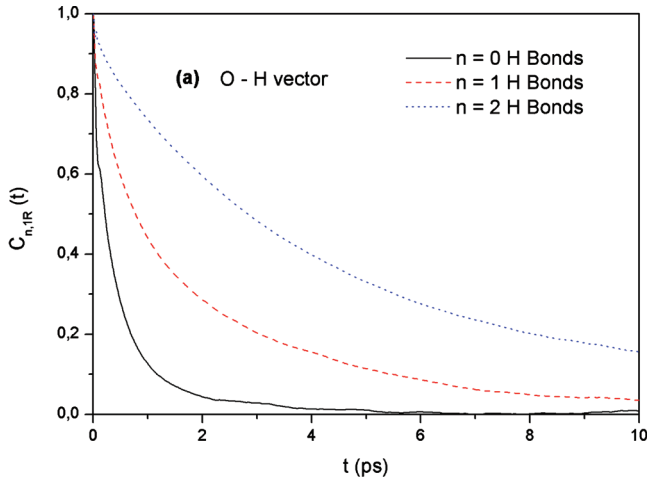

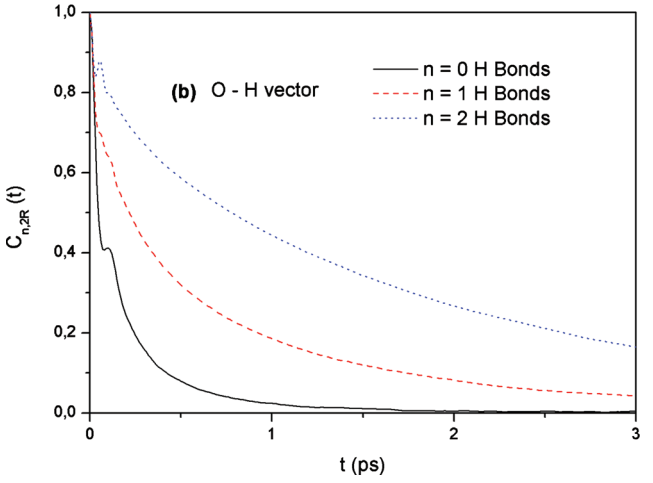

FIG. 10. First and second order Legendre reorientational correlation functions for the O–H vector of EtOH molecules corresponding to the initial HB states $n=0,1,2$ (for EtOH–EtOH H bonds).

ecules affects strongly their reorientational dynamics. We may observe that as the values of n increase the reorientational tcf's $C_{n,\ell R}(t)$ decay slower, thus resulting to larger values of reorientational correlation times $\tau_{n,\ell R}$. The dependence of the calculated reorientational times $\tau_{n,\ell R}$ on the HB state n of the EtOH molecules is depicted in Fig. 11. From this figure we may see that the first order Legendre reorientational times $\tau_{n,1-R}$ of the C_1-C_2 and C_2-O vectors exhibit a linear dependence on the HB state n and those corresponding to the O–H vector exhibit a small deviation from linearity. These deviations from linearity become more apparent in the case of the second order *Legendre* reorientational times, where this nonlinear behavior is observed for all the vectors and is more pronounced in the case of the reorientation of the O–H vector, which is more strongly affected by HB interactions. Possibly this rapid increase in the reorientation time of the O–H vector as we are going from HB state $n=1$ to $n=2$ is also related to the higher intermittent lifetime of the $n=2$ HB state. This behavior indicates that the effect of the initial $n=2$ HB network on reorientational dynamics lasts for a larger time scale, thus leading to a larger retardation of these dynamics. It is also interesting to note that in the case of EtOH molecules which were initially HB free ($n=0$ HB state) the calculated reorientational times $\tau_{0,\ell-R}$ are very similar for all the intramolecular vectors, whereas as the value of n increases we observe a different effect of the HB state on these reorientational motions, resulting to a much slower reorientation of the O–H vectors in comparison to the C_2-O and C_1-C_2 vectors. The strong effect of the HB state on the O–H reorientational dynamics is also reflected on the short-time scale dynamics ($\sim$0–0.1 ps), where the characteristic local minima observed at short time scales for typical associated HB liquids such as water and alcohols, reflecting the librational motions due to HB interactions, are much more pronounced for higher n values. All these observations clearly signify the strong effect of the HB state of the EtOH molecules on their reorientational dynamics, and that the reorientational motions of different intramolecular vectors are affected differently by the HB state of the molecules.

It is interesting to note here that in previously reported experimental NMR study[25] of methanol-CO_2 mixtures the authors reported ^{13}C spin-lattice relaxation times of methanol. When the authors in that study tried to analyze the behavior of ^{13}C spin-lattice relaxation times of the methanol molecules assuming no aggregation between them, their approach was quite inadequate in describing the experimentally obtained experimental results. Furthermore, they observed that the obtained ^{13}C spin-lattice relaxation times could be

TABLE VI. Legendre reorientational times for several intramolecular unit vectors of EtOH molecules as a function of their initial HB state.

	C_1-C_2 vector	
	$\tau_{n,1R}$ (ps)	$\tau_{n,2R}$ (ps)
$n=0$	0.54	0.22
$n=1$	1.28	0.29
$n=2$	2.15	0.42
	C_2-O vector	
	$\tau_{n,1R}$ (ps)	$\tau_{n,2R}$ (ps)
$n=0$	0.65	0.24
$n=1$	2.25	0.51
$n=2$	4.11	1.11
	O–H vector	
	$\tau_{n,1R}$ (ps)	$\tau_{n,2R}$ (ps)
$n=0$	0.50	0.17
$n=1$	1.94	0.63
$n=2$	4.78	1.66

interpreted in terms of a HB model of spin-rotation relaxations coupled with the formation of hydrogen bonds to produce alcohol oligomers. These results are in agreement with our findings in the present study, where we have predicted that each EtOH molecule does not form more than one or two hydrogen bonds and that the reorientational relaxation of EtOH molecules is significantly affected by the presence of hydrogen bonds. Since it is well known that spin-lattice and reorientational relaxation times are closely related to each other, these findings that the presence of hydrogen bonds affects spin-lattice relaxation dynamics are completely in accordance with our results concerning the effect of the HB state of EtOH molecules on their reorientational relaxation. Moreover, it is interesting to note that the authors in that study predicted very small differences between CO_2 spin-lattice relaxation times in the mixtures with methanol and in pure CO_2. In our previous MD simulation study[36] we had predicted as well that the calculated reorientational times of CO_2 molecules in the mixture, which exhibit much weaker HB interactions with EtOH than the EtOH ones, are quite close to those corresponding to pure CO_2 at similar thermodynamic conditions. This behavior was also observed in the case of CO_2-CH_4 mixtures, where HB interactions are completely absent.[49] All these findings clearly signify that the presence of hydrogen bonds between the EtOH molecules strongly affects their reorientational dynamics.

D. Translational dynamics

In the present treatment we have also focused on single translational dynamics of EtOH molecules, namely, how they are affected by the HB state of the EtOH molecules. In this case, we have calculated the hydrogen velocity tcf's using the well-known relation

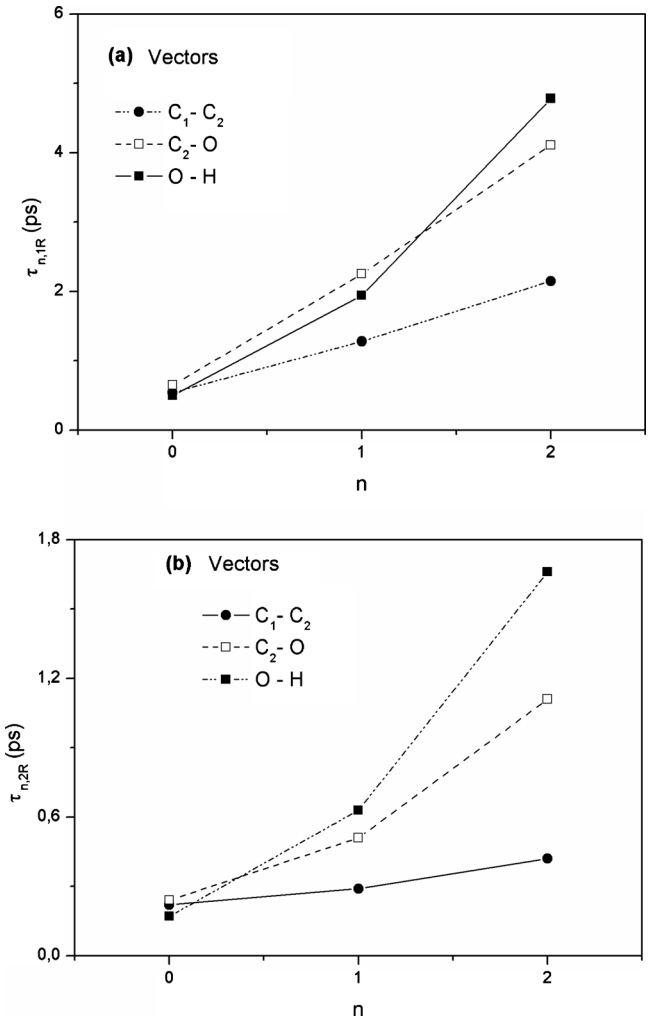

FIG. 11. First and second order Legendre reorientational times as a function of the HB state of EtOH molecules (for EtOH–EtOH H bonds).

$$C_v^H(t) = \frac{\langle \vec{v}_H(0) \cdot \vec{v}_H(t) \rangle}{\langle \vec{v}_H(0)^2 \rangle}. \tag{19}$$

The corresponding spectral densities $S_v^H(\omega)$ have been also calculated by performing a Fourier transform on the $C_v^H(t)$ tcf's,

$$S_v^H(\omega) = \int_0^\infty \cos(\omega \cdot t) \cdot C_v^H(t) \cdot dt. \tag{20}$$

The $S_v^H(\omega)$ have been calculated by numerical integration using a Bode rule, after applying a Hanning window to the calculated atomic velocity tcf's. The results obtained are depicted in Fig. 12. It is interesting to note that the average $S_v^H(\omega)$ exhibits two peaks located at 242 and 547 cm^{-1}. These peaks could be a result of the dihedral angle intramolecular vibrations of ethanol as well as of intermolecular librational motions due to HB interactions between the EtOH molecules. These findings motivated us to further investigate the question "how the HB state of the EtOH molecules affects the shape of the power spectrum and the position of the peaks observed in the average $S_v^H(\omega)$." Thus, we first calculated the functions[54]

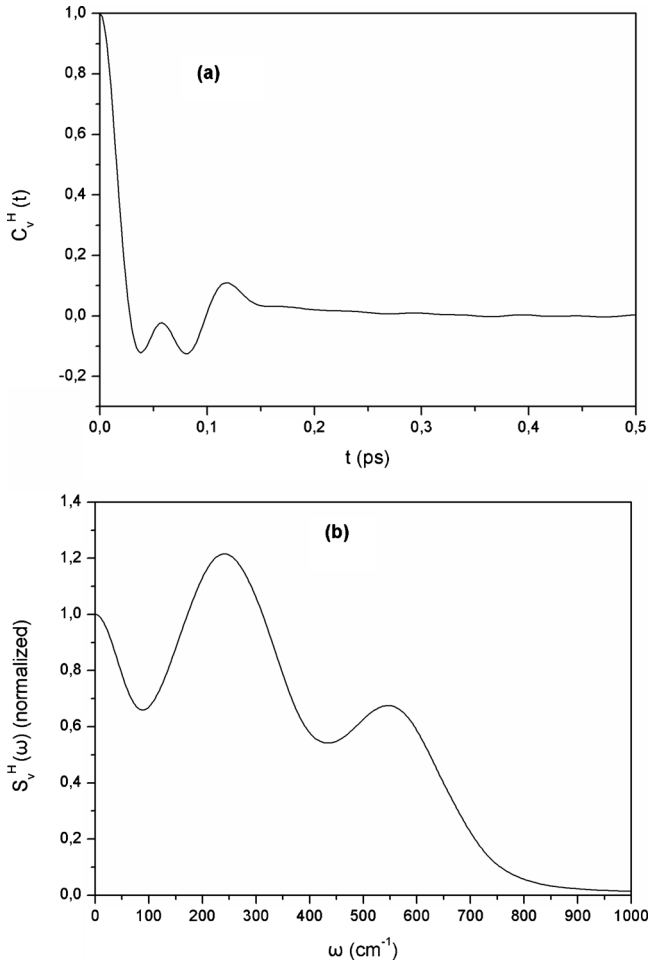

FIG. 12. Average hydrogen atomic velocity tcf and the corresponding spectral density for the EtOH molecules in the system.

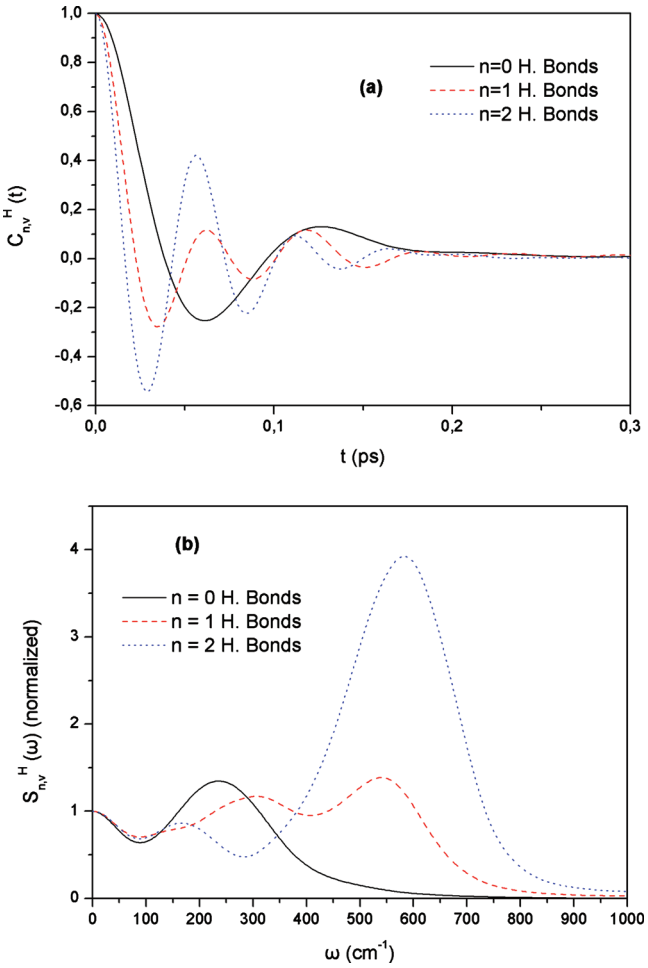

FIG. 13. Hydrogen atomic velocity tcf's and the corresponding spectral density EtOH molecules corresponding to the initial HB states $n=0,1,2$ (for EtOH–EtOH H bonds).

$$C_{n,v}{}^H(t) = \frac{\langle \vec{v}_H(0) \cdot \vec{v}_H(t) \cdot \Theta_n(0) \rangle}{\langle \vec{v}_H(0)^2 \cdot \Theta_n(0) \rangle}. \tag{21}$$

The function $\Theta_n(t)$ has already been defined in Eq. (17). After calculating these tcf's we obtained the corresponding spectral densities $S_{n,v}{}^H(\omega)$ using the relation

$$S_{n,v}{}^H(\omega) = \int_0^\infty \cos(\omega \cdot t) \cdot C_{n,v}{}^H(t) \cdot dt. \tag{22}$$

The calculated tcf's $C_{n,v}{}^H(t)$ and the corresponding spectral densities $S_{n,v}{}^H(\omega)$ for the initial HB states $n=0,1,2$ are presented in Fig. 13. From this figure we may clearly see that the initial HB state of the EtOH molecules affects significantly their translational dynamics. If we inspect carefully the behavior of $C_{n,v}{}^H(t)$, we may see that as the value of n increases we observe a more pronounced dumped oscillator behavior with negative minima and positive maxima. This behavior indicates that the local HB network perturbates significantly the translational motion of EtOH molecules due to its effect on the intermolecular librational motions of these molecules. This may be more clearly seen by inspecting the calculated spectral densities $S_{n,v}{}^H(\omega)$, where it is observed that the function $S_{n,v}{}^H(\omega)$ for $n=0$ exhibits only one peak located at 236 cm^{-1}. In the case of $n=1$ the spectral density $S_{n,v}{}^H(\omega)$ exhibits two peaks located at 305 and 539 cm^{-1} and in the case of $n=2$ exhibits two peaks located at 167 and 581 cm^{-1}, respectively. The fact that the second peak located at higher frequencies appears only in the case of initially hydrogen bonded EtOH molecules indicates that this peak is related to the intermolecular libration motions due to HB interactions between the EtOH molecules. This is a very important observation, which could not be extracted from the average spectral density $S_v{}^H(\omega)$, since the average tcf $C_v{}^H(t)$ is a weighted sum of the functions $C_{n,v}{}^H(t)$,

$$C_v{}^H(t) = \sum_n (f_n \cdot C_{n,v}{}^H(t)), \tag{23}$$

where f_n is the fraction of EtOH molecules having n EtOH–EtOH hydrogen bonds. Therefore, the average spectral density could be obtained by the equation

$$\begin{aligned} S_v{}^H(\omega) &= \int_0^\infty \left(\cos(\omega \cdot t) \cdot \sum_n (f_n \cdot C_{n,v}{}^H(t)) \right) \cdot dt \\ &= \sum_n \left(f_n \cdot \int_0^\infty \cos(\omega \cdot t) \cdot C_{n,v}{}^H(t) \cdot dt \right) \\ &= \sum_n (f_n \cdot S_{n,v}{}^H(\omega)). \end{aligned} \tag{24}$$

Therefore, due to this weighted sum the average spectral

density exhibits two distinct peaks due to the contributions of hydrogen bonded molecules and the absence of the second peak in the case of the $n=0$ HB state could be revealed only by calculating the function $S_{0,v}{}^{H}(\omega)$. This is also the reason why the second peak intensity of the average spectral density $S_{v}{}^{H}(\omega)$ is lower than the intensity of the first peak, namely, due to the high contribution of HB free molecules in the overall function, whereas in the case of $n=2$ we may observe a significantly higher intensity for the second peak of $S_{2,v}{}^{H}(\omega)$. The observation of this significantly higher second peak intensity in the case of $n=2$ signifies clearly the strong effect of HB interactions on the librational motion of the EtOH molecules and is very difficult to be detected in a real far-IR experiment.[55,56]

IV. CONCLUDING REMARKS

In the framework of the present study, the HB structure and dynamics in binary sc solutions of EtOH in CO_2 ($X_{EtOH} \sim 0.1$) have been thoroughly investigated using MD simulation techniques. The results obtained have revealed that the number of hydrogen bonds between EtOH molecules is significantly larger than that corresponding to the EtOH–CO_2 ones. Moreover, the existence of possible EDA EtOH–CO_2 dimers has been also investigated and it has been found that the EDA interactions between EtOH and CO_2 molecules in the mixture are possibly more important than the HB ones. More specifically, we have found that $\langle n_{HB}\rangle_{EtOH-EtOH} > \langle n_{EDA}\rangle_{EtOH-CO_2} > \langle n_{HB}\rangle_{EtOH-CO_2}$, which could be used as a guide to classify the importance of these interactions in the mixture.

Furthermore, a more detailed analysis on the stability of these interactions has been presented in terms of the dynamic behavior of these interacting pairs in the mixture. According to our analysis the HB lifetimes are significantly larger in the case of EtOH–EtOH hydrogen bonds in comparison with those corresponding to the EtOH–CO_2 ones, especially in the case of intermittent dynamics. Also we have observed that the correlation between EDA dimers is stronger than in the case of the hydrogen bonded ones. All these results indicate that the EtOH–EtOH HB dimers are the most stable in the system and the EDA EtOH–CO_2 dimers are more stable than the EtOH–CO_2 HB ones. Additionally, the calculation of residence dynamics for the first solvation shell of EtOH and CO_2 molecules has revealed that the residence times of EtOH inside an EtOH solvation shell are much larger in comparison to all the other calculated lifetimes, whereas the lifetimes of CO_2 inside a CO_2 solvation shell are the smallest ones. This result seems to be reasonable taking into account all the aforementioned findings concerning HB dynamics.

Since our results signified a strong EtOH–EtOH interaction in the mixture, we extended our investigations in order to study the effect of the HB state of the EtOH molecules on their single reorientational and translational dynamics. The results obtained have depicted a significant effect of the initial HB state of the EtOH molecules on their reorientational dynamics. We may observe that as the value of hydrogen bonds per EtOH molecule n increases, the reorientational tcf's $C_{n,\ell R}(t)$ decay slower, thus resulting to larger values of the corresponding reorientational correlation times $\tau_{n,\ell R}$. Concerning the dependence of the calculated reorientational times $\tau_{n,\ell R}$ on the HB state n of the EtOH molecules, the first order Legendre reorientational times $\tau_{n,1-R}$ of the C_1-C_2 and C_2-O vectors exhibit a linear dependence on the HB state n, while those corresponding to the O–H vector exhibit a small deviation from linearity. This deviation from linearity becomes more apparent in the case of the second order Legendre reorientational times and for all the unit vectors defined above. However, this nonlinear behavior is more pronounced in the case of the reorientation of the O–H vector and possibly is related to the stronger effect of HB interactions on O–H reorientation. In the case of translational dynamics it has been found that the initial HB state of the EtOH molecules affects very significantly their translational motion due to its effect on the intermolecular librational motions of these molecules. The calculation of the spectral densities $S_{n,v}{}^{H}(\omega)$ of the hydrogen velocity tcf's $C_{n,v}{}^{H}(t)$ for the different HB states of the EtOH molecules has shown that in the case of hydrogen bonded molecules ($n=1,2$) the spectral densities exhibit a peak, which is not present in the case of initially HB free molecules ($n=0$). This is a very important observation, since it reveals that this peak, which is also present in the average spectral density $S_{v}{}^{H}(\omega)$, is probably related to the intermolecular libration motions due to HB interactions between the EtOH molecules. All these findings signify very clearly the strong effect of the local HB network on the translational and librational dynamics of EtOH.

ACKNOWLEDGMENTS

E.G. gratefully acknowledges financial support from the Direcció General de Recerca de la Generalitat de Catalunya (Grant No. 2009SGR-1003) and from the Ministerio de Ciencia e Innovación of Spain (Grant No. FIS2009-13641-CO2-01).

[1] M. Besnard, T. Tassaing, Y. Danten, J. M. Andanson, J. C. Soetens, F. Cansell, A. Loppinet-Serani, H. Reveron, and C. Aymonier, J. Mol. Liq. **125**, 88 (2006).
[2] X. Zhang, B. Han, Z. Hou, J. Zhang, Z. Liu, T. Jiang, J. He, and H. Li, Chem.-Eur. J. **8**, 5107 (2002).
[3] S. Sala, T. Tassaing, N. Ventosa, Y. Danten, M. Besnard, and J. Veciana, ChemPhysChem **5**, 243 (2004).
[4] J. M. Dobbs, J. M. Wong, R. J. Lahiere, and K. P. Johnston, Ind. Eng. Chem. Res. **26**, 56 (1987).
[5] R. M. Lemert and K. P. Johnston, Ind. Eng. Chem. Res. **30**, 1222 (1991).
[6] G. S. Gurdial, S. J. Macnaughton, D. L. Tomasko, and N. R. Foster, Ind. Eng. Chem. Res. **32**, 1488 (1993).
[7] B. Guan, Z. Liu, B. Han, and Y. Han, J. Supercrit. Fluids **14**, 213 (1999).
[8] Y. Koga, Y. Iwai, Y. Hata, M. Yamamoto, and Y. Arai, Fluid Phase Equilib. **125**, 115 (1996).
[9] M. Roth, J. Chromatogr., A **1037**, 369 (2004).
[10] C. Boukouvalas, K. Magoulas, and D. Tassios, Sep. Sci. Technol. **33**, 387 (1998).
[11] D. Ekeberg and A. M. Jablonska-Jentoft, J. Am. Soc. Mass Spectrom. **18**, 2173 (2007).
[12] B. Wang, B. X. Han, T. Jiang, Z. F. Zhang, Y. Xie, W. J. Li, and W. Z. Wu, J. Phys. Chem. B **109**, 24203 (2005).
[13] H. P. Li, B. X. Han, J. Liu, L. Gao, Z. S. Hou, T. Jiang, Z. M. Liu, X. G. Zhang, and J. He, Chem.-Eur. J. **8**, 5593 (2002).
[14] Z. Huang, Y. C. Chiew, W.-D. Lu, and S. Kawi, Fluid Phase Equilib. **237**, 9 (2005).
[15] H.-K. Bae, J.-H. Jeon, and H. Lee, Fluid Phase Equilib. **222–223**, 119 (2004).

[16] P. Lalanne, S. Rey, F. Cansell, T. Tassaing, and M. Besnard, J. Supercrit. Fluids **19**, 199 (2001).
[17] T. Tassaing, P. Lalanne, S. Rey, F. Cansell, and M. Besnard, Ind. Eng. Chem. Res. **39**, 4470 (2000).
[18] G. Chatzis and J. Samios, Chem. Phys. Lett. **374**, 187 (2003).
[19] J. M. Stubbs and J. I. Siepmann, J. Chem. Phys. **121**, 1525 (2004).
[20] H. Li and M. Maroncelli, J. Phys. Chem. B **110**, 21189 (2006).
[21] H. D. Lüdemann and L. Chen, J. Phys.: Condens. Matter **14**, 11453 (2002).
[22] J. L. Fulton, G. G. Yee, and R. D. Smith, J. Am. Chem. Soc. **113**, 8327 (1991).
[23] D. M. Pfund, J. L. Fulton, and R. D. Smith, in *Supercritical Fluid Engineering Science Fundamentals and Applications*, ACS Symposium Series Vol. 514, edited by J. F. Brennecke and E. Kiran (American Chemical Society, Washington, DC, 1993).
[24] J. L. Fulton, G. G. Yee, and R. D. Smith, in *Supercritical Fluid Engineering Science Fundamentals and Applications*, ACS Symposium Series Vol. 514, edited by J. F. Brennecke and E. Kiran (American Chemical Society, Washington, DC, 1993).
[25] C. M. V. Taylor, S. Bai, C. L. Mayne, and D. M. Grant, J. Phys. Chem. B **101**, 5652 (1997).
[26] M. Kanakubo, T. Aizawa, T. Kawakami, O. Sato, Y. Ikushima, K. Hatakeda, and N. Saito, J. Phys. Chem. B **104**, 2749 (2000).
[27] D. L. Goldfarb, D. P. Fernández, and H. R. Corti, Fluid Phase Equilib. **158–160**, 1011 (1999).
[28] R. L. Smith, Jr., C. Saito, S. Suzuki, S.-B. Lee, H. Inomata, and K. Arai, Fluid Phase Equilib. **194–197**, 869 (2002).
[29] D. S. Bulgarevich, T. Sato, T. Sugeta, K. Otake, M. Sato, M. Uesugi, and M. Kato, J. Chem. Phys. **108**, 3915 (1998).
[30] P. Lalanne, T. Tassaing, Y. Danten, F. Cansell, S. C. Tucker, and M. Besnard, J. Phys. Chem. A **108**, 2617 (2004).
[31] H. Pöhler and E. Kiran, J. Chem. Eng. Data **42**, 384 (1997).
[32] G. S. Gurdial, N. R. Foster, S. L. J. Yun, and K. D. Tilly, in *Supercritical Fluid Engineering Science Fundamentals and Applications*, ACS Symposium Series Vol. 514, edited by J. F. Brennecke and E. Kiran (American Chemical Society, Washington, DC, 1993).
[33] X. Zhang, B. Han, L. Shi, H. Li, and G. Yang, J. Supercrit. Fluids **24**, 193 (2002).
[34] K. D. Tilly, N. R. Foster, S. J. Macnaughton, and D. L. Tomasko, Ind. Eng. Chem. Res. **33**, 681 (1994).
[35] M. Saharay and S. Balasubramanian, J. Phys. Chem. B **110**, 3782 (2006).
[36] I. Skarmoutsos, D. Dellis, and J. Samios, J. Chem. Phys. **126**, 224503 (2007).
[37] W. Xu, J. Yang, and Y. Hu, J. Phys. Chem. B **113**, 4781 (2009).
[38] Y. Danten, T. Tassaing, and M. Besnard, J. Phys. Chem. A **106**, 11831 (2002).
[39] J. G. Harris and K. H. Young, J. Phys. Chem. **99**, 12021 (1995).
[40] W. L. Jorgensen, J. Phys. Chem. **90**, 1276 (1986).
[41] D. Dellis, M. Chalaris, and J. Samios, J. Phys. Chem. B **109**, 18575 (2005).
[42] I. Skarmoutsos and E. Guardia, J. Phys. Chem. B **113**, 8887 (2009).
[43] I. Skarmoutsos and E. Guardia, J. Phys. Chem. B **113**, 8898 (2009).
[44] J. A. Padró, L. Saiz, and E. Guardia, J. Mol. Struct. **416**, 243 (1997).
[45] L. Saiz, J. A. Padro, and E. Guardia, Mol. Phys. **97**, 897 (1999).
[46] L. Saiz, E. Guardia, and J. A. Padro, J. Chem. Phys. **113**, 2814 (2000).
[47] I. Skarmoutsos and J. Samios, J. Chem. Phys. **126**, 044503 (2007).
[48] J. E. Adams and A. Siavosh-Haghighi, J. Phys. Chem. B **106**, 7973 (2002).
[49] I. Skarmoutsos and J. Samios, J. Mol. Liq. **125**, 181 (2006).
[50] H. J. C. Berendsen, J. P. M. Postma, W. F. van Gunsteren, A. DiNola, and J. R. Haak, J. Chem. Phys. **81**, 3684 (1984).
[51] J. P. Ryckaert, G. Ciccotti, and H. J. C. Berendsen, J. Comput. Phys. **23**, 327 (1977).
[52] D. Paschek and A. Geiger, MOSCITO 4.140, University of Dortmund, Dortmund, Germany, 2007.
[53] T. Schnabel, A. Srivastava, J. Vrabec, and H. Hasse, J. Phys. Chem. B **111**, 9871 (2007).
[54] I. Skarmoutsos and E. Guardia, J. Chem. Phys. **132**, 074502 (2010).
[55] J. Samios, U. Mittag, and T. Dorfmüller, Mol. Phys. **56**, 541 (1985).
[56] T. Dorfmüller, J. Samios, and U. Mittag, Chem. Phys. **107**, 397 (1986).